Aerosols and the Residual Clear-sky Insolation Discrepancy

Thomas P. Charlock 1 t.p.charlock@larc.nasa.gov
Fred G. Rose 2 f.g.rose@larc.nasa.gov
David A. Rutan 2 d.a.rutan@larc.nasa.gov

1 Mail Stop 420, NASA Langley Research Center, Hampton VA 23681
tel: 1-757-864-5687 fax: 1-757-864-7996

2 Analytical Services and Materials, Inc., One Enterprise Parkway, Hampton VA 23666
tel: 1-757-827-4649(Rose) -4629(Rutan) fax: 1-757-766-9601

group URL: www-cave.larc.nasa.gov/cave/

Extended Abstract for ARM Science Team Meeting
Atlanta, 19-22 March 2001

Abstract

The "clear-sky insolation discrepancy" surfaced a few years ago: Several well-regarded theoretical simulations (sound radiative transfer codes and carefully measured inputs for them) produced values for clear sky shortwave (SW) insolation that exceeded measurements to 20-30 Wm-2. Now, by both carefully screening (Long-Ackerman) the radiometer observations and including the record of the newly installed Eppley Black and White (B&W) pyranometer, we find theory exceeding observations by means of –2.1 Wm-2 (total), -7.3 Wm-2 (direct horizontal), and 5.2 Wm-2 (diffuse) for 500 half-hourly observations during January-December 2000 at the SGP (Southern Great Plains) CF (Central Facility) C01 site. For moderate values of AOT, the aerosol forcing to surface insolation is considerably greater than the (now reduced) discrepancy of theory and observations.

The perspective from a detailed look at the time series is less rosy. The fine agreement in time mean for the direct horizontal, the component of flux which can be most confidently measured, is produced by compensation: Theory exceeds measurement for one period, and measurement exceeds theory for another. Results with permutations of Cimel versus MFRSR (Multifilter Rotating Shadowband Radiometer) for AOT (Aerosol Optical Thickness), the use of different broadband instruments, and confining to periods of agreement between duplicate measurements tell a similar story; and cannot be satisfactorily explained as due to minor H2O effects which were not in the present simulation. With the current generation of observations, we approach a limit for matching with simulations of the direct beam in an extended time series. This suggests that adjustments, for example, of soot fraction (here assumed 10% with a modified Fu-Liou code) to routinely assess aerosol absorption via comparison with the diffuse beam face the same barrier. The accurate assessment of anthropogenic forcing to the absorption of SW by the atmosphere yet remains beyond the grasp of climate science.

At TOA (top of the atmosphere) for reflected SW flux, simulations using surface albedos observed at the C01 site exceed the Terra (satellite) CERES (Clouds and the Earth’s Radiant Energy System) "ERBE-like" (Earth Radiation Budget Experiment) ES8 (ERBE Science) archival product by a mean of 27.0 Wm-2 for a set of 44 footprints during 2000 which were carefully screened as cloud free. When the identical footprints were compared with calculations based

on surface albedos measured by radiometers at the adjacent E13 site, the broadband reflected from computations then exceeded CERES by 13.2 Wm-2.

1. Introduction

For the past few years, ARM has been plagued by a discrepancy between computed and observed values of broadband SW insolation at the surface under clear (cloud free) conditions. Charlock and Alberta (1996), Kato et al. (1997), and Halthore et al. (1998) reported that computations exceeded measurements by 20-30 Wm-2. The finding was widespread at SGP but not universal: Zender et al. (1997) reported agreement within 10 Wm-2 when using observations from the special Radiation Atmospheric Measurement System (RAMS) pyranometer at SGP; Wild et al. (1999) found consistency of observations and theory using data from Kipp and Zonen pyranometers in Europe; Kato et al. (1999) found no significant discrepancy for a molecular (largely aerosol free) atmosphere at an elevated site in Hawaii.

It now appears that much of the discrepancy was due to errors in the broadband observations. The Eppley Precision Spectral Pyranometer (PSP), which has been frequently used at SGP for SW measurements, has a thermal offset. The PSP responds slightly to thermal infrared radiation, as well as to SW. If the offset caused by thermal radiation is not accounted for, the PSP readily yields a NEGATIVE value for SW insolation at night (Bush et al., 2000; Haeffelin et al, 2000; Dutton et al., 2001). As the shaded PSP has been part of the standard ARM package for the measurement of insolation by the component sum method recommended by the Baseline Surface Radiation Network (BSRN), many ARM observations of insolation prior to the year 2000 are biased low; these have been referred to as “SIROS”, “SIRS” and “BSRN” in the literature (and the attribution of one battery of instruments as “BSRN”, which has been the jargon of some, is disputed by others). The thermal offset in some Kipp and Zonen pyranometers and in the Eppley Black and White (B&W) instrument is much reduced or even negligible. Dutton et al. (2001) developed an adjustment procedure for the PSP record using simultaneous measurements from the Precision Infrared Radiometer (PIR), which is often collocated with the PSP. The Dutton et al. (2001) method compares favorably with a more rigorous modification of the PSP itself (Haeffelin et al., 2000). Alberta and Charlock (1999) implemented the bulk of the Dutton et al. adjustment to CAGEX (CERES ARM GEWEX) Version 2, which spans the SGP CF for Fall 1996 (GEWEX is the Global Energy and Water Cycle Experiment), as have Rutan et al. (2001) for the on-line CERES ARM Validation Experiment (CAVE).

An Eppley B&W was deployed at ARM site C01 in June 1999. As the B&W is not susceptible to thermal offset, we have confined the observations used in this work to the year 2000. For comparison with the C01 site, we use data from the collocated E13 radiometers. The shaded pyranometer at E13 is an Eppley PSP, here adjusted for thermal offset using a monthly regression to night records from the PSP and the net radiation reported at the PIR detector. Dutton et al. (2001) includes an additional (and generally smaller) correction based on the PIR dome and body temperatures.

Why the fuss over closure of observations with theory for broadband SW under clear skies at SGP? One goal is the establishment of consistency between the radiation measurements, radiative transfer theory, and observationally based inputs for the radiative transfer calculations. Mlawer et al. (2000) have reported substantial agreement of spectral measurements and theory from 350-1100 nm. While Mlawer et al. (2000) used a more limited domain than here, they were able to conclude that the small discrepancies of measurement and theory had no sharp spectral features that could be ascribed to inadequacies in line strengths, etc., in the simulation. The aerosol single scattering albedo which Mlawer et al. (2000) tuned in order to approach closure was surprisingly low, however. Aerosol optical properties loom as the possible kink in closure. An earlier study (Fu et al., 1998) showed no significiant

discrepancies in the broadband that could be ascribed to uncertainties in the amount or optical properties of water vapor.

Successful closure of observations and theory for broadband SW under clear skies would afford us with the capability to monitor direct aerosol forcing. Improvements in satellite remote sensing may be close to providing such monitoring capability at TOA. The big question in direct aerosol forcing is the impact on atmospheric absorption through the single scattering albedo. Closure at both surface and TOA would yield the atmospheric absorption. Here we attempt to close at the surface, using a full year of data at the SGP CF. This is a pilot study which could be extended to few score sites worldwide with data from the online CAVE (see URL www-cave.larc.nasa.gov/cave/).

2. Radiative Transfer Calculations

We use a modified form of the Fu-Liou radiative transfer model (Fu and Liou, 1993) as presently employed in the Surface and Atmospheric Radiation Budget (SARB; Charlock et al., 1997, and Rose et al., 1997) component of CERES (Wielicki et al., 1996) and maintained as a "point and click" feature on the URL srbsun.larc.nasa.gov/sarb/sarb.html. The code has been modified to include 10 bands for O3 and Rayleigh scattering (0.2-0.7 um) and now approximates the effects of solar radiation beyond 4 um. The Chou and Suarez (1999) treatment of SW absorption by CO2, O2, and by a weak visible band of H2O is included. Compared with the version of Fu-Liou used by Charlock and Alberta (1996), the new code has more atmospheric absorption, and it shifts slightly more radiation from the direct into the diffuse beam. Changes in the code, as well as in the observations, have reduced the discrepancy between theory and measurement.

The optical properties of aerosols are here parameterized as 90% continental (d'Almeida et al., 1991) and 10% soot (Hess et al., 1998), wherein single scattering albedo and asymmetry factor vary with the relative humidity (RH) reported in the sounding. Observations of spectral aerosol optical thickness (AOT) from the AERONET (Holben et al., 1998) Cimel are used from 340-1020 nm; these set the AOT in the bands of the Fu-Liou code by using a smooth fit that is logarithmic in both AOT and wavelength (i.e., a log-log plot). At longer (>1020 nm) and shorter (<340 nm) wavelengths, the fit is constrained by the models of d'Almeida et al. (1991) and Hess et al. (1998). Temperature and humidity soundings were taken from the standard weekday ARM radiosondes. Precipitable water (PW) from the SGP surface-based Microwave Radiometer (MWR) was used to scale the radiosonde PW and provide half-hourly updated values. Daily ozone profiles were obtained from the CERES Meteorology Ozone and Aerosol (MOA) files, which are based on the NOAA Stratospheric Monitoring Group Ozone Blended Analysis (SMOBA) of Yang et al. (2000). In midlatitudes SMOBA uses data from the daylight and nadir viewing SBUV/2 (Solar Backscattered Ultraviolet) satellite instrument.

Radiative transfer calculations were made for the ARM SGP using the mean cosine of solar zenith angle (SZA) appropriate for a 30 minute interval under clear skies. Clouds were screened using the Long and Ackerman (2000) algorithm, which is applied to the temporally intensive broadband record at the surface. Calculations were made only for those 30-minute intervals that were separated from a radiosonde launch by less than 24 hours. The surface spectral albedo (Rutan and Charlock, 1997, 1999) is taken from the measured 30-minute broadband albedo at the respective surface site, as adjusted with the spectral shape of milo which was measured during the CERES ARM Radiation Experiment (CARE) at SGP (for global maps see the URL tanalo.larc.nasa.gov:8080/surf_htmls/SARB_surf.html). Calculations used the surface albedos, respectively, from the C01 and E13 Solar and Infrared Radiation Stations (SIRS), which are collocated. Calculations for C01 and E13 used identical profiles of AOT and PW.

3. Comparison of Observations and Calculations

Table 1 shows the mean bias (model minus observation) and aerosol forcing (theoretical flux with AOT minus theoretical flux without AOT) at SGP during 2000. As noted earlier, the advantage of the year 2000 is the installation of the Eppley B&W pyranometers for a more accurate diffuse and total SW flux at C01. For comparing the modeled and observed insolation, we have a sample of 500 intervals each of 30 minutes. The direct normal is the beam normal to the sun as observed by the Eppley Normal Incidence Pyrheliometer (PIR). Diffuse is measured by the shaded Eppley (offset corrected PSP at E13 or B&W at C01). The observed value for direct horiztonal is the mean of the minute-by-minute product of the direct normal and cosine of the solar zenith angle (SZA).

Table 1 Bias (Model-Obs) and Aerosol Forcing in Wm-2 at SGP during 2000

	Model - Obs		Sample	Aerosol
	E13	C01	N	Forcing
Surface				
Direct normal	-4.1	-10.0	500	-131.3
Diffuse	6.7	5.2	500	58.6
Total	3.3	-2.1	500	-27.5
Direct horizontal =(dir norm)*cosSZA	-3.4	-7.3	500	-86.1
TOA reflected	13.2	27.0	44	<- this N is tiny!

The theoretical mean total aerosol forcing at the surface has a moderate value at –27.5 Wm-2 and results from larger forcings of opposite sign due to the diffuse (58.6 Wm-2) and direct horizontal (-86.1 Wm-2). The theoretical aerosol forcing is produced by both natural and anthropogenic aerosols. The forcing in Table 1 is a daytime only, clear-sky quantity. While it would be smaller for the 24 hour mean, its value at the surface would still greatly exceed the greenhouse (infrared) forcing produced by anthropogenic gases. The Intergovernmental Panel on Climate Change (IPCC, 1995) estimates anthropogenic greenhouse forcing as only 2-3 Wm-2 at the tropopause and much less at the surface. Anthropogenic greenhouse forcing is very difficult to observe; but because the relevant gases are mostly well mixed, adequately measured, and understood spectroscopically, theoretical forcings *for the infrared greenhouse* should be reliable worldwide. In contrast, IPCC notes that the direct aerosol forcing is highly uncertain on a global basis. It is thus gratifying to note that for each row of Table 1, the absolute magnitude of the aerosol forcing exceeds the absolute magnitude of the difference between model and observation by about a factor of 10.

Figure 1 allows more careful examination of the differences of model minus observations for direct normal, diffuse (adjusted PSP for observations), total and direct horizontal SW at surface site E13 as time series. Each panel shows the mean difference of model and observations and the (standard deviation) in paretheses. While the differences for each component, such as –4.1 Wm-2 for the direct, are small for the annual mean, there is much scatter. The differences of

model and observation are seen to vary considerably within a given (clear-sky) day. Further, there appear to be low frequency variations in the differences of model and observation. The bias for the diffuse at E13 is fairly small between days ~280-320 (second panel in Fig. 1). Is the small bias during days 280-320 due to a fortuitous guess in single scattering albedo, from our selection of a 10% soot burden? Or is it due to compensation by another error?

The top panel in Figure 1 for the direct normal shows the start of a signficant period of error for the direct normal during the same days 280-320. Errors in the direct normal are more readily judged as significant because the direct normal is measured by the Normal Incidence Pyrheliometer (NIP), which is the most highly regarded instrument in the SIRS battery. The jump in the bias for direct normal (-15 Wm-2 near day 260 versus +20 Wm-2 near day 290) could be due, hypothetically, to a Cimel AOT which rapidly and incorrectly reports a decrease in aerosol loading; this would tend to push the direct normal upwards in the Fu-Liou model (the jump); and it would pull the diffuse downwards in the Fu-Liou model (the fall in the second panel of Fig. 1). Features around days 280-320 in the direct normal (first panel) and diffuse (second panel) are similar for site C01 (Figure 2). The direct normal jumps in both Figures 1 and 2 suggests that this is not a simple case of abrupt changes in only the single scattering albedo of the aerosol (i.e., a vexing of our assumption for a constant fraction of 10% soot). The spectral variation of the AOT reported by Cimel during fall 2000 reveals abrupt kinks around 670 nm (not shown); this could be an instrument anomaly; or an effect due to the Cimel processing algorithm, which uses climatological O3 loadings.

Aerosol forcing is defined as the theoretical flux with aerosols minus the theoretical flux without aerosols. In Figure 3 (4), the aerosol forcing is shown in red for site E13 (C01) as a scatter plot versus observed AOT. The forcing to total SW at the surface (third panels in Figs. 3 and 4) is linear with AOT. As a marker of the fidelity of the theoretical forcing (red), the scatter plots also depict the bias as model minus observation (black) versus AOT. For large values of AOT, the forcings have much larger absolute magnitudes than do the biases of model minus observation; this was also the case for the mean forcings and biases in Table 1. The forcings in Table 1 may be regarded as reliable estimates for the daylight mean, clear-sky direct aerosol forcing to the surface for year 2000 at the SGP CF. The modest success of this estimate is accompanied by the caveat that it is a result of our selection of 10% as the portion of soot in the computation. A 10% increase (decrease) in the percentage of soot would perturb the diffuse and total surface SW by roughly 10 Wm-2, and the resulting magnitude of the total surface forcing would no longer exceed that of the bias by a factor of 10. A further caveat is illustrated by the second panels of Figs. 3 and 4, wherein the bias (black marks) for diffuse flux shows a variation with AOT. For both the diffuse bias (second panel, black) and total bias (third panel, black) are slightly positive at low AOT and negative at high AOT. If the same plot is shown versus PW (not shown) rather than versus AOT, we find no such systematic variation of the bias with PW. This aspect of the bias for diffuse and total versus AOT would be consistent with an aerosol composition that has a larger fraction of soot at low AOT and a smaller fraction of soot at high AOT. Mlawer et al. (2000) also reported a case wherein more aerosol absorption was needed to establish closure at low AOT. While we have assumed a constant fraction of soot, the absorbing efficiency of the aerosol is consistent with a variable fraction of soot (or of some other absorber, such as large dust particles).

What about the bias at the TOA? For an investigation at TOA, we use CERES footprints that have been subset and collocated with the ground site (i.e., Rose et al., 2001), as available online at CAVE (Rutan et al., 2001). The CERES data are instantaneous, but here we have adjusted them to correspond to represent half-hourly means, as with the surface data; and the Long-Ackerman method is used to identify clear intervals with surface radiometer data. Table 1 notes biases of 13.2 Wm-2 and 27.0 Wm-2 using, respectively, the highly local surface albedos measured at the E13 and C01 sites and CERES ES-8 data. Figs. 5 (E13) and 6 (C01) compare computations for reflected SW flux (top panel) and broadband albedo (lower panel) at TOA with Edition 2 ES-8

observations from CERES on the Terra spacecraft. The E13 and C01 radiometers are both at the CF. As the difference in computed TOA flux between the sites (27.0-13.2=13.8 Wm-2) is almost as large as the mean bias (20.1 Wm-2), we infer that it will be difficult to "validate" retrievals of surface albedo for the large CERES footprints (~20 km) with radiometers mounted on 10 m towers; the surface albedo over land is too heterogeneous. The sample size (N=44) for this comparison with CERES is much smaller than the sample for the surface (N=500). Caution is needed on serveral accounts when interpreting CERES clear-sky ES-8 data. First, the TOA flux inferred from a scanner-based radiance from CERES is not a direct measurement (Wielicki et al., 1996). The TOA fluxes are estimated from Angular Distribution Models (ADM) which are valid for the statistical mean; an individual retrieval is quite noisy. Second, the archived ES-8 fluxes are based completely on coarse resolution CERES data. The crucially important scene identification process, which is needed to select the proper ADM for inversion from radiance to flux, does not employ a high spatial resolution cloud imager in ES-8. And the ES-8 ADMs are dated. More advanced CERES Single Satellite Footprint (SSF) products do use a cloud imager for scene identification, and they are based on more comprehensive ADMs from a Rotating Azimuth Plane Scanner (RAPS) that was not available in ERBE. Clear sky SSFs are now available from the URL eosweb.larc.nasa.gov, but not yet for year 2000.

4. Discussion

Table 1 shows that for the mean of 500 half-hourly, clear-sky daylight samples during 2000, the biases for broadband surface SW at SGP is small when using either the E13 or C01 set of radiometers; for each component, the aerosol forcing is an order of magnitude larger than bias. The mean total biases are 3.3 Wm-2 at E13 and –2.1 Wm-2 at C01, a separation of only 5.4 Wm-2. Most of the separation is produced by different readings of direct normal from the NIPs, which have a calibration procedure that is superior to those of other radiometers deployed by ARM. The community's calibration standard for broadband diffuse is not as rigorous; and there is no formal international protocol for calibration of the narrowband photometers (i.e., Cimel and MFRSR) that measure spectral AOT. The surface forcing produced by the chosen, constant composition (90% continental and 10% soot) for the aerosol is regarded as a reasonable estimate for the mean. We hesitate, however, to suggest that this procedure yields a realistic description of temporal variations in forcing. In an attempt to close on temporal variations in aerosol forcing, we could adjust the aerosol composition daily, requiring closer agreement of model and observation. We have used this approach earlier, including geostationary satellite data to close on atmospheric absorption. While this course will continue to be pursued with broadband CERES data, it is not expected to fully resolve discrepancies like the odd jump in the direct normal bias from day 260 to 290. The odd jump is probably an error in aerosol instrumentation or processing of the instrument record. Given the inherent "ADM noise" from the satellite, one is more confident in its application to a time mean, rather than a small number of observations. Small, long-term variations in aerosols could have dramatic effects on climate. At a given site, a long-term change in forcing could well be due to a series of short episodes with unexpected variations in aerosol compositon. A higher quality instrument record would permit us to confidently monitor the changes in the direct forcing of aerosols at a significant number of sites.

References

Alberta, T. L., and T. P. Charlock, 1999: A comprehensive resource for the investigation of shortwave fluxes in clear conditions: CAGEX Version 3. Proceedings of the AMS Tenth Conference on Atmospheric Radiation, Madison WI (June 28 – July 2, 1999), 279-282.

Bush, B. C., F. P. J. Valero, A. Sabrina Simpson, and L. Bignone, 2000: Characterization of thermal effects in pyranometers: A data correction algorithm for improved measurement of surface insolation. J. of Atmos. Ocean. Tech., 17, 165-175.

Charlock, T. P., and T. L. Alberta, 1996: The CERES/ARM/GEWEX Experiment (CAGEX) for the retrieval of radiative fluxes with satellite data. Bull. Amer. Meteor. Soc., 77, 2673-2683.

Charlock, T. P., F. G. Rose, D. A. Rutan, T. L. Alberta, D. P. Kratz, L.H. Coleman, G. L. Smith, N. Manalo-Smith, and T. D. Bess, 1997: Compute Surface and Atmospheric Fluxes (System 5.0), CERES Algorithm Theoretical Basis Document. 84 pp. See http://asd-www.larc.nasa.gov/ATBD/.

Chou, M.-D., and M. J. Suarez, 1999: A solar radiation parameterization for atmospheric studies. NASA/TM-1999-104606, Vol. 15, 40 pp.

d'Almeida, G., P. Koepke, and E. P. Shettle, 1991: Atmospheric Aerosols - Global Climatology and Radiative Characteristics. A. Deepak Publishing, Hampton, Virginia. 561 pp.

Dutton, E. G., J. J. Michalsky, T. Stoffel, B. W. Forgan, J. Hickey, D. W. Nelson, T. L. Alberta, and I. Reda, 2001: Measurement of broadband diffuse solar irradiance using current commercial instrumentation with a correction for thermal offset errors. J. Atmos. Ocean. Tech., 18, 297-314.

Fu, Q., G. Lesins, J. Higgins, T. Charlock, P. Chylek, and J. Michalsky, 1998: Broadband water vapor absorption of solar radiation tested using ARM data. Geophys. Res. Lett., 25, 1169-1172.

Fu, Q., and K.-N. Liou, 1993: Parameterization of the radiative properties of cirrus clouds. J. Atmos. Sci., 50, 2008-2025.

Haeffelin, M., S. Kato, A. M. Smith, K. Rutledge, T. Charlock, and J. R. Mahan, 2001: Determination of the thermal offset of the Eppley Precision Spectral Pyranometer. Appl. Opt., 40, 472-484.

Halthore, R. N., S. Nemesure, S. E. Schwartz, D. G. Imre, A. Berk, E. G. Dutton, and M. H. Bergin, 1998: Models overestimate diffuse clear-sky surface irradiance: A case for excess atmospheric absorption. Geophys. Res. Lett., 25, 3591-3594.

Hess, M., P. Koepke, and I. Schult, 1998: Optical Properties of Aerosols and Clouds: The software package OPAC. Bull. Amer. Meteor. Soc., 79, 831-844.

Holben, B. N., T. F. Eck, I. Slutsker, D. Tanre, J. P. Buis, A. Setzer, E. Vermote, J. A. Reagan, Y. J. Kaufman, T. Nakajima, F. Lavenu, I. Jankowiak, and A. Smirnov, 1998: AERONET – A federated instrument network and data archive for aerosol characterization. Remote Sens. Environ., 66, 1-16.

Intergovernmental Panel on Climate Change (IPCC), 1995: Climate Change 1995. The Science of Climate Change. Houghton, J. T., et al., Eds., Cambridge University Press. 572 pp.

Kato, S., T. P. Ackerman, E. E. Clothiaux, J. H. Mather, G. R. Mace, M. Wesley, F. Murcray, and J. Michalsky, 1997: Uncertainties in modeled and measured clear-sky surface shortwave irradiances. J. Geophys. Res., 102, 25,881-25,898.

Kato, S., T. P. Ackerman, E. G. Dutton, N. Laulainen, and N. Larson, 1999: A comparison of modeled and measured surface shortwave irradiance for a molecular atmosphere, J. Quant. Spectrosc. Radiat. Transfer., 61, 493-502.

Long, C. N., and T. P. Ackerman, 2000: Identification of clear skies from broadband pyranometer measurements and calculation of downwelling shortwave cloud effects. J. Geophys. Res., 105, 15,609-15,626.

Mlawer, E. J., P. D. Brown, S. A. Clough, L. C. Harrison, J. J. Michalsky, P. W. Kiedron, and T. Shippert, 2000: Comparison of spectral direct and diffuse solar irradiance measurments and calculations for cloud free conditions. Geophys. Res. Lett., 27, 2653-2656.

Rose, F. G., T. P. Charlock, and D. A. Rutan, 2001: Impact of Clouds on the Atmospheric Absorption of SW - Comparing Theory and Observation at SGP. Poster at the ARM Science Team Meeting, Atlanta, 19-23 March 2001.

Rose, F., T. Charlock, D, Rutan, and G. L. Smith, 1997: Tests of a constrainment algorithm for the surface and atmospheric radiation budget. Proceedings of the Ninth Conference on Atmospheric Radiation, Long Beach (Feb. 2-7, 1997), AMS, 466-469.

Rutan, D., and T. Charlock, 1997: Spectral reflectance, directional reflectance, and broadband albedo of the earth's surface. Proceedings of the Ninth Conference on Atmospheric Radiation, Long Beach (Feb. 2-7, 1997), AMS, 466-469.

Rutan, D., and T. Charlock, 1999: Land surface albedo with CERES broadband observations. Proceedings of the Tenth Conference on Atmospheric Radiation, Madison WI (28 June – 2 July), 1999, AMS, 208-211.

Rutan, D. A., T. P. Charlock, and F. G. Rose, 2001: The CERES ARM Validation Experiment (CAVE). Poster at the ARM Science Team Meeting, Atlanta, 19-23 March 2001.

Wielicki, B. A., B. R. Barkstrom, E. F. Harrison, R. B. Lee, G. L. Smith, and J. E. Cooper, 1996: Clouds and the Earth's Radiant Energy System (CERES): An Earth Observing System Experiment. Bull. Amer. Meteor. Soc., 77, 853-868.

Wild, M., 1999: Discrepancies between model-calculated and observed shortwave atmospheric absorption in areas with high aerosol loadings. J. Geophys. Res., 104, 27,361-27,373.

Yang, S.-K., S. Zhou, and A. J. Miller, 2000: SMOBA: A 3-dimensional daily ozone analysis using SBUV/2 and TOVS measurements. This document is available at the following URL: www.cpc. ncep.gov/products/stratosphere/SMOBA/smoba_doc.html

Zender, C. S., B. Bush, S. K. Pope, A. Bucholtz, W. D. Collins, J. T. Kiehl, F. P. Valero, and J. Vitko, Jr., 1997: Atmospheric absorption during the Atmospheric Radiation Measurement (ARM) Enhanced Shortwave Experiment (ARESE). J. Geophys. Res., 102, 29,901-29916.

Figure Captions

Figure 1 Difference of model and observations (Fu-Liou model minus OBS) for broadband SW in Wm-2 versus time at ARM SGP site E13. Clear-sky data in half-hourly intervals. Panels display direct normal, diffuse (shaded PSP adjusted for thermal offset), total (sum of direct horizontal and diffuse), and direct horizontal (product of direct normal and cosSZA).

Figure 2 Difference of model and observations (Fu-Liou model minus OBS) for broadband SW in Wm-2 versus time at ARM SGP site C01. Clear-sky data in half-hourly intervals. Panels display direct normal, diffuse (shaded B&W), total (sum of direct horizontal and diffuse), and direct horizontal (product of direct normal and cosSZA).

Figure 3 Aerosol forcing (model with aerosol minus model without aerosol) in red and model bias (model with aerosol minus observations) in black for broadband SW in Wm-2 versus time at ARM SGP site E13. Clear sky-data in half-hourly intervals. Panels display direct normal, diffuse (shaded PSP adjusted for thermal offset), total (sum of direct horizontal and diffuse), and direct horizontal (product of direct normal and cosSZA).

Figure 4 Aerosol forcing (model with aerosol minus model without aerosol) in red and model bias (model with aerosol minus observations) in black for broadband SW in Wm-2 versus time at ARM SGP site C01. Clear sky-data in half-hourly intervals. Panels display direct normal, diffuse (shaded B&W), total (sum of direct horizontal and diffuse), and direct horizontal (product of direct normal and cosSZA).

Figure 5 Reflected SW at TOA from Fu-Liou model versus CERES ES8 Terra satellite observations. Model inputs include surface albedo from radiometer at site E13. Clear-sky only (clouds screened with surface radiometer data). SW in Wm-2 (upper panel) and as albedo (lower panel).

Figure 6 Reflected SW at TOA from Fu-Liou model versus CERES ES8 Terra satellite observations. Model inputs include surface albedo from radiometer at site C01. Clear-sky only (clouds screened with surface radiometer data). SW as flux in Wm-2 (upper panel) and as albedo (lower panel).

0301..ARM_SGP_E13 : CIMEL(7) SMOOTH AOTs: Jan2000-Dec2000 Cave Flux Data
Sonde T(z),Q(z): MWRPW : SMOBA O3(z) : CLEAR C.Long<0.02

Direct Normal
N= 500 Model-Obs= -4.1 (12.7)

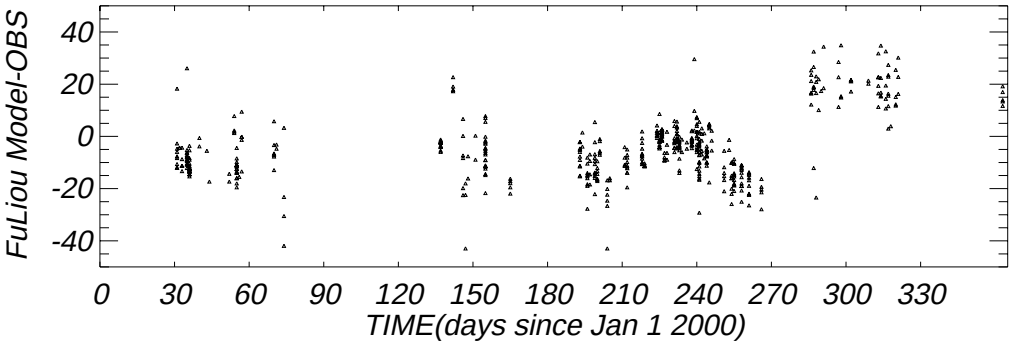

Diffuse(PSP adj)
N= 500 Model-Obs= 6.7 (8.1)

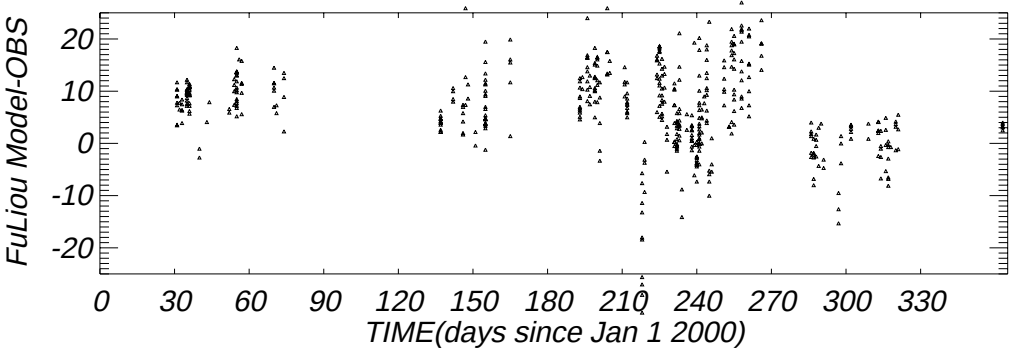

Total SW
N= 500 Model-Obs= 3.3 (7.7)

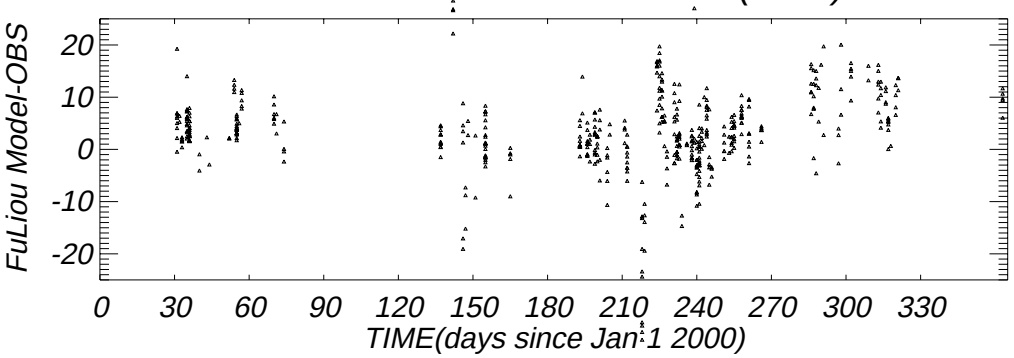

Direct Horizontal SW
N= 500 Model-Obs= -3.4 (8.6)

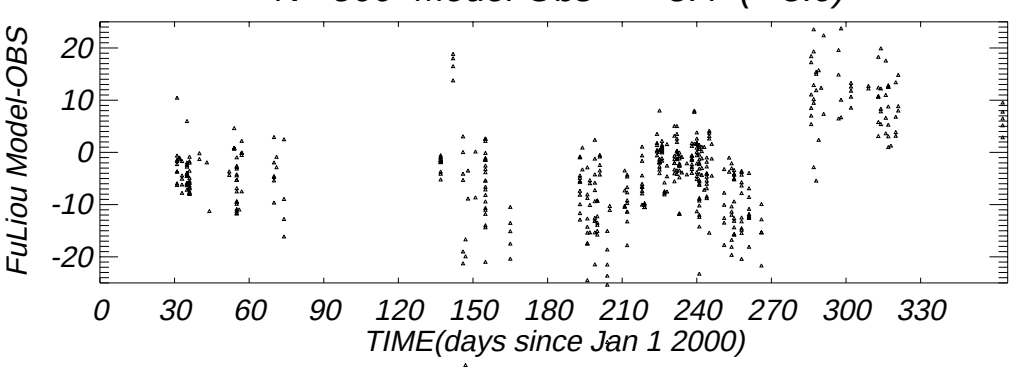

0301..ARM_SGP_C01 : CIMEL(7) SMOOTH AOTs: Jan2000-Dec2000 Cave Flux Data
Sonde T(z),Q(z): MWRPW : SMOBA O3(z) : CLEAR C.Long<0.02

Direct Normal
N= 500 Model-Obs= -10.0 (11.0)

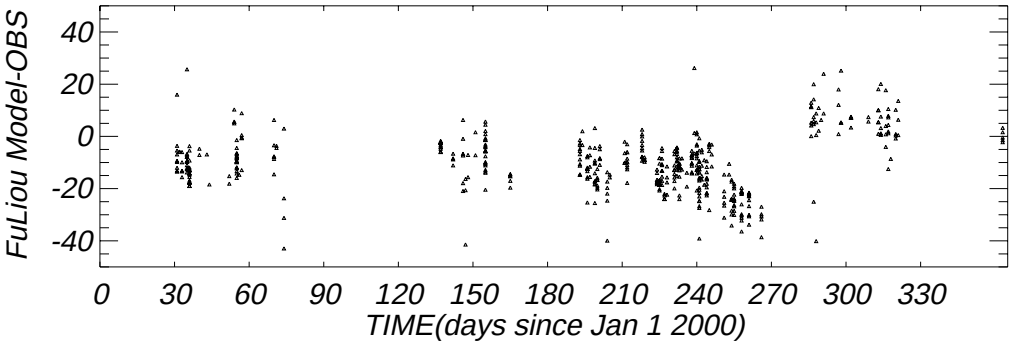

Diffuse(BW)
N= 500 Model-Obs= 5.2 (7.6)

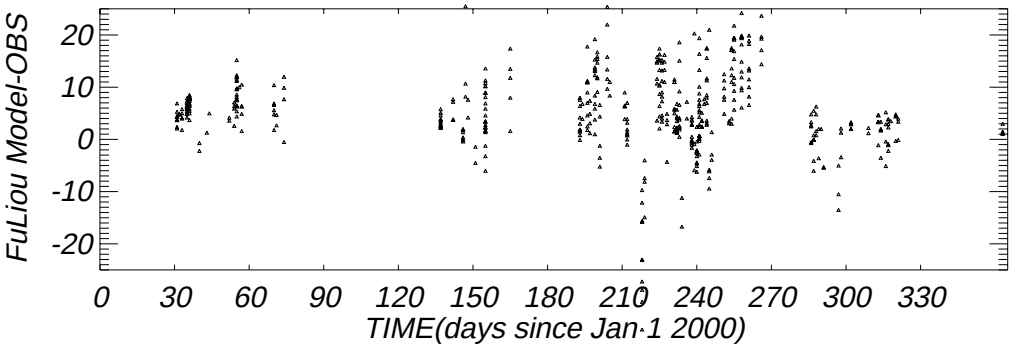

Total SW
N= 500 Model-Obs= -2.1 (6.6)

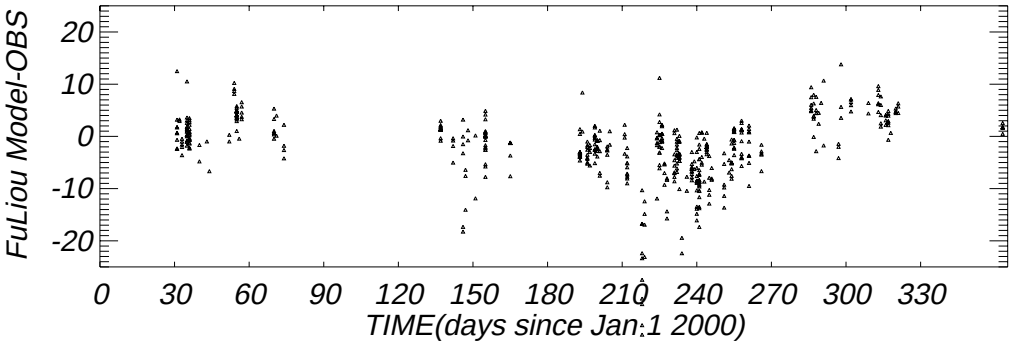

Direct Horizontal SW
N= 500 Model-Obs= -7.3 (8.1)

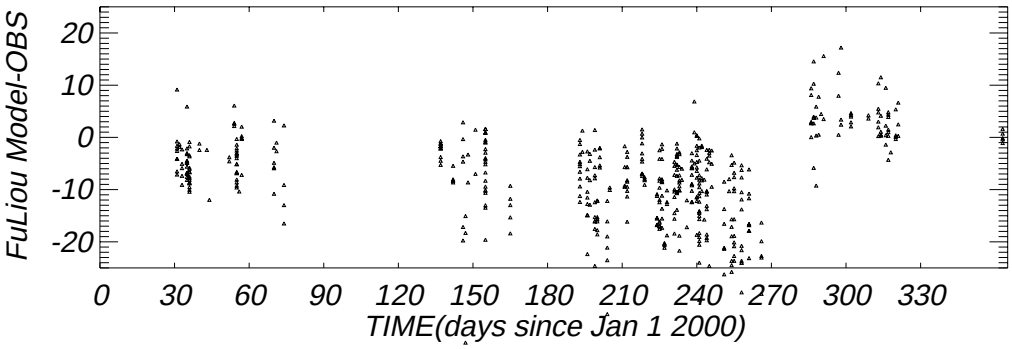

0301..AEROSOL FORCING
ARM_SGP_E13 : CIMEL(7) SMOOTH AOTs: Jan2000-Dec2000 Cave Flux Data
Sonde T(z),Q(z): MWRPW : SMOBA O3(z) : CLEAR C.Long<0.02
N= 500

Direct Normal [Wm-2]
Model-Obs= -4.1 (12.7) Aerosol Forcing= -131.3 (54.4)

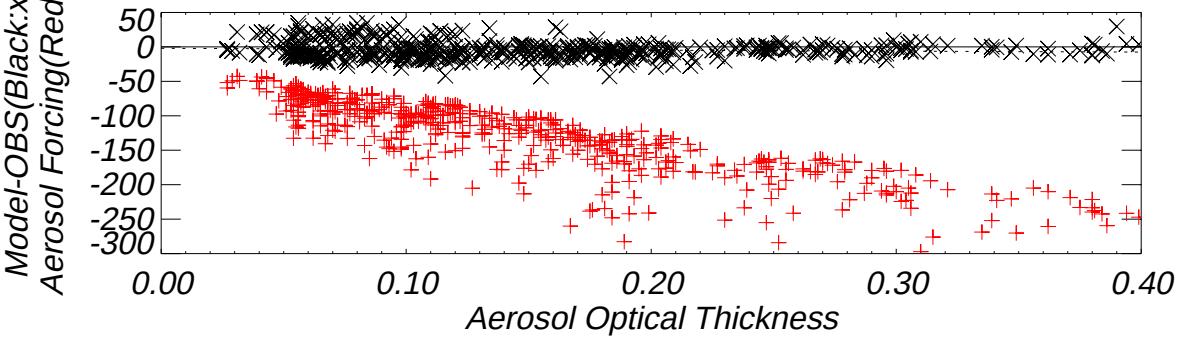

Diffuse(adj) [Wm-2]
Model-Obs= 6.7 (8.1) Aerosol Forcing= 58.6 (31.5)

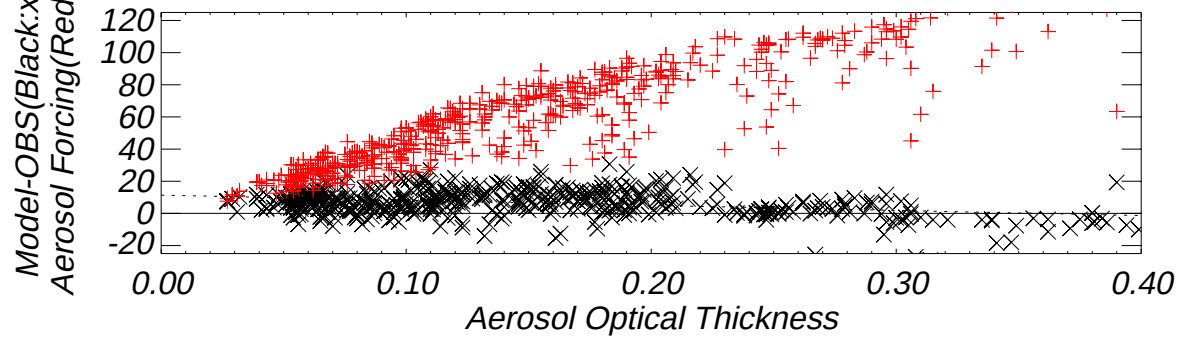

Total SW [Wm-2]
Model-Obs= 3.3 (7.7) Aerosol Forcing= -27.5 (13.5)

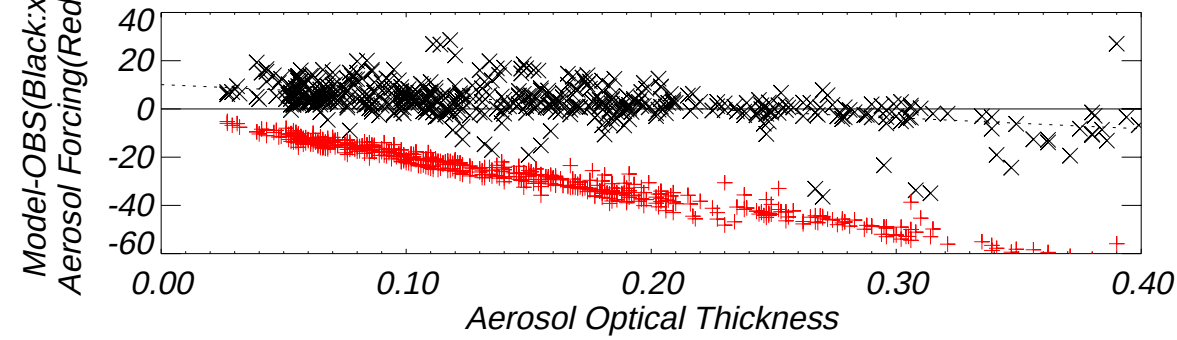

Direct Horizontal SW [Wm-2]
Model-Obs= -3.4 (8.6) Aerosol Forcing= -86.1 (44.6)

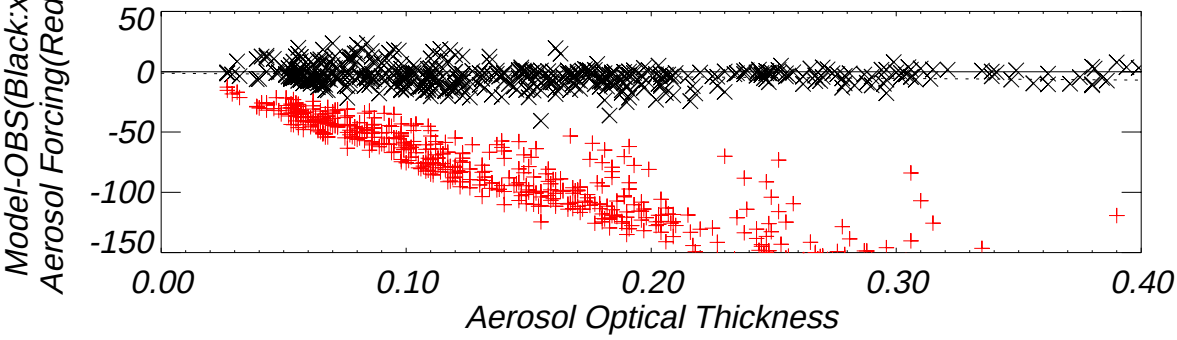

0301..AEROSOL FORCING
ARM_SGP_C01 : CIMEL(7) SMOOTH AOTs: Jan2000-Dec2000 Cave Flux Data
Sonde T(z),Q(z): MWRPW : SMOBA O3(z) : CLEAR C.Long<0.02
N= 500

Direct Normal [Wm-2]
Model-Obs= -10.0 (11.0) Aerosol Forcing= -131.3 (54.4)

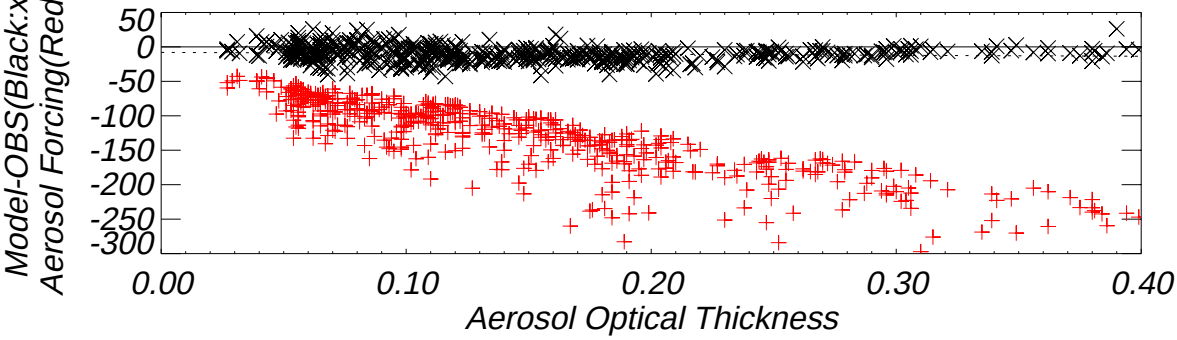

Diffuse(adj) [Wm-2]
Model-Obs= 5.2 (7.6) Aerosol Forcing= 58.8 (31.7)

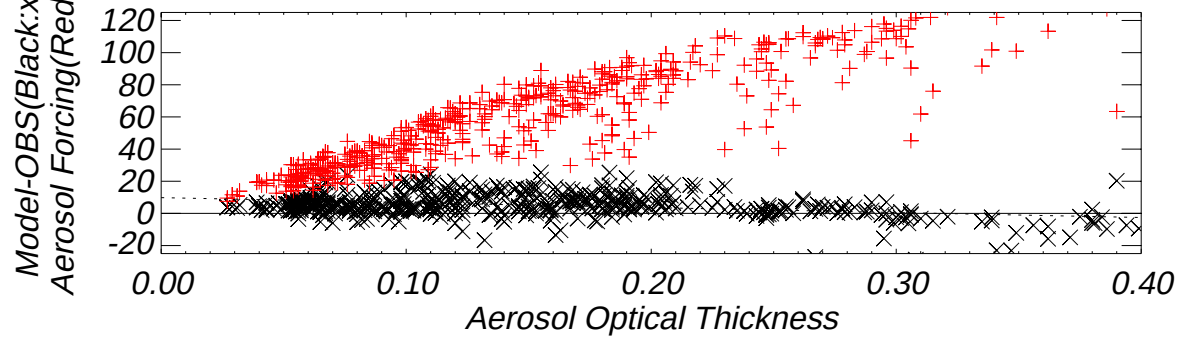

Total SW [Wm-2]
Model-Obs= -2.1 (6.6) Aerosol Forcing= -27.3 (13.4)

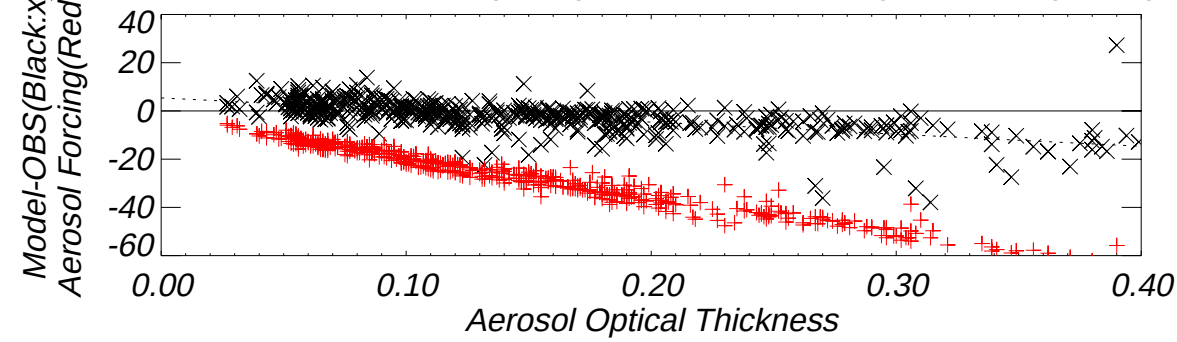

Direct Horizontal SW [Wm-2]
Model-Obs= -7.3 (8.1) Aerosol Forcing= -86.1 (44.6)

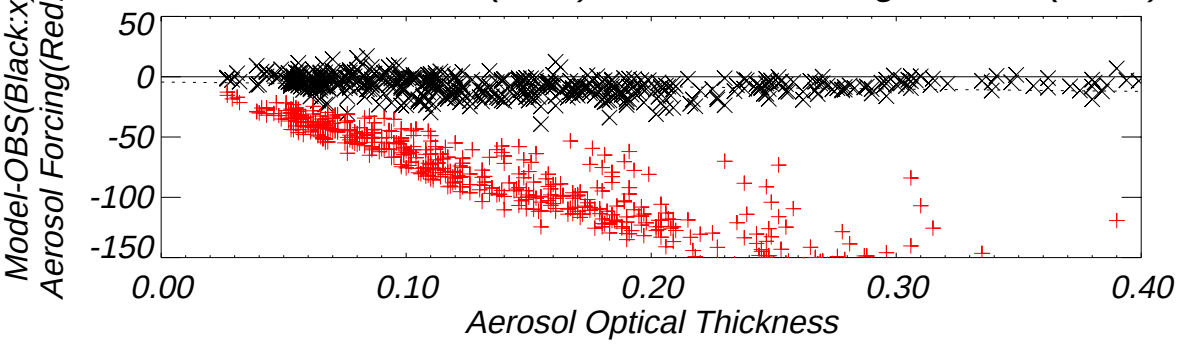

0301..ARM_SGP_E13 : CIMEL(7) SMOOTH AOTs: Jan2000-Dec2000 Cave Flux Data
Sonde T(z),Q(z): MWRPW : SMOBA O3(z) : CLEAR C.Long<0.02

TOA REFLECTED SW (Erbe-like TERRA ES8_Ed2)
N= 44 Model-Obs= 13.2 (17.3)

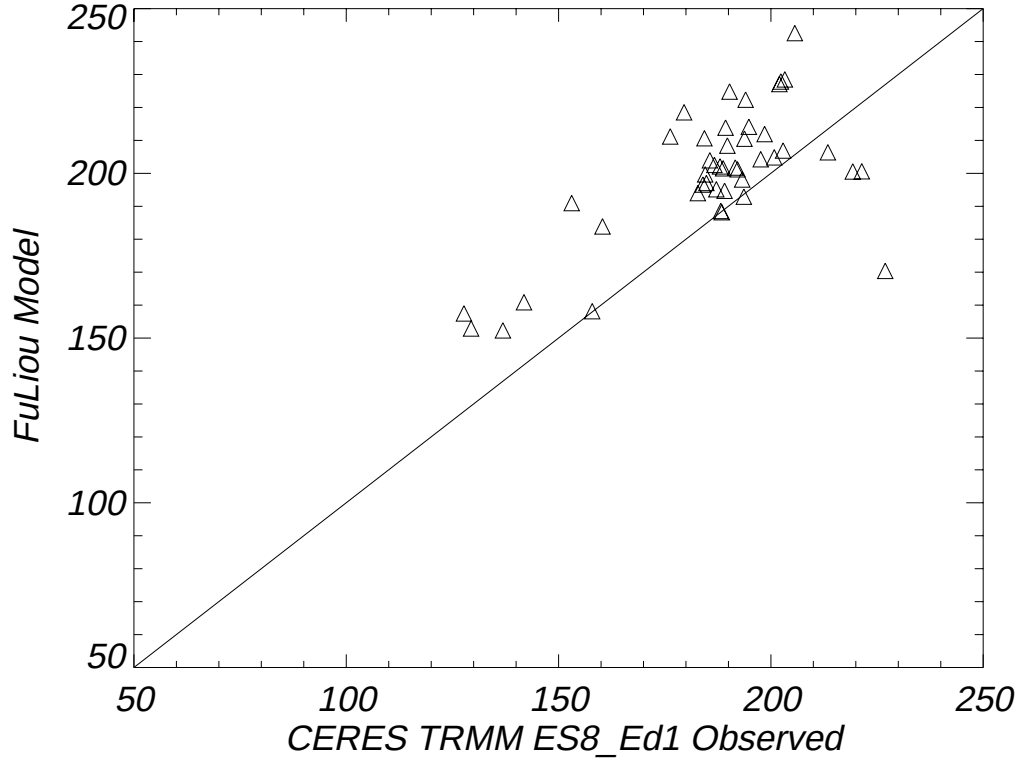

TOA ALBEDO (Erbe-like TERRA ES8_Ed2)
N= 44 Model-Obs= 0.012 (0.018)

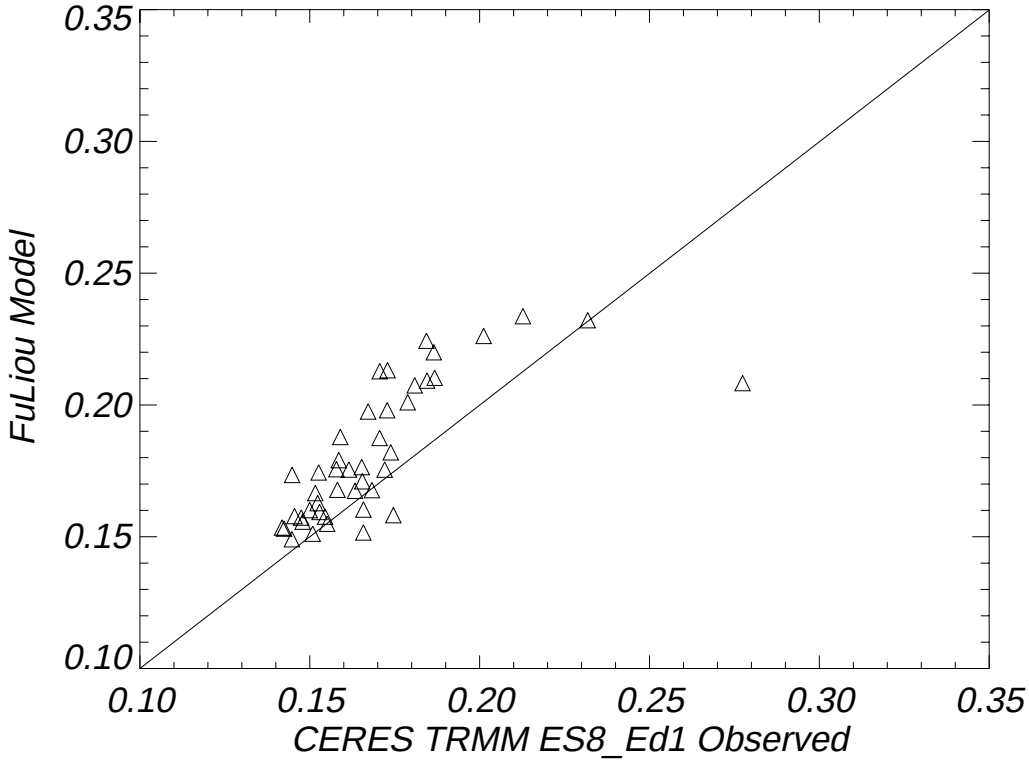

0301..ARM_SGP_C01 : CIMEL(7) SMOOTH AOTs: Jan2000-Dec2000 Cave Flux Data
Sonde T(z),Q(z): MWRPW : SMOBA O3(z) : CLEAR C.Long<0.02

TOA REFLECTED SW (Erbe-like TERRA ES8_Ed2)
N= 44 Model-Obs= 27.0 (19.9)

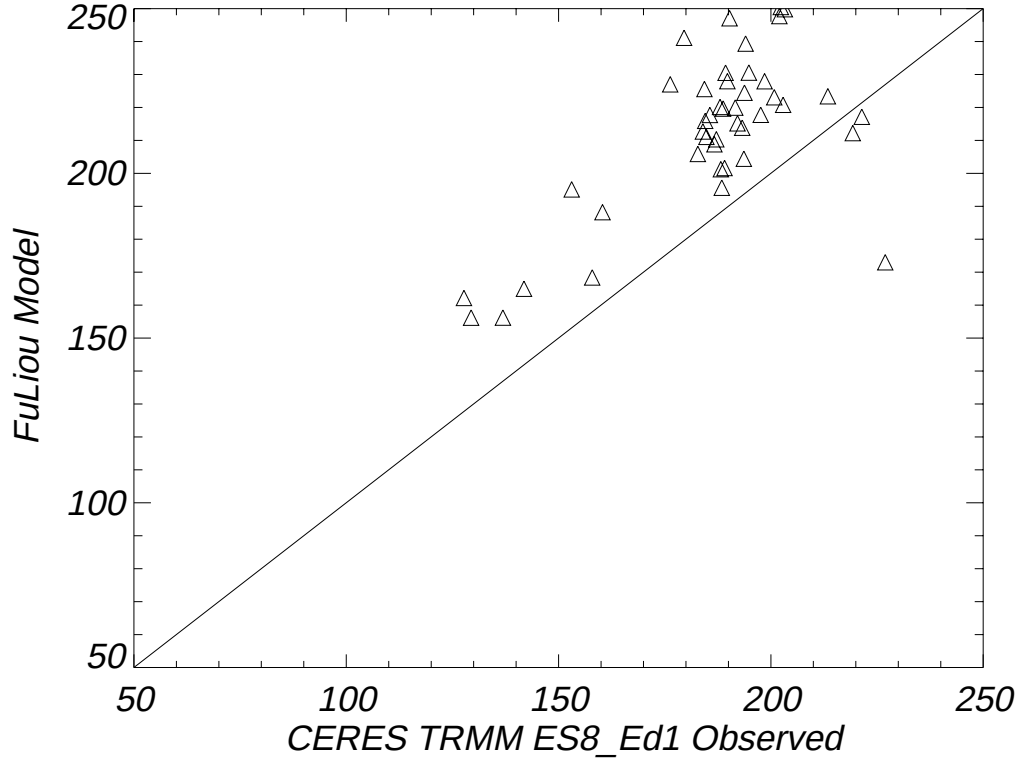

TOA ALBEDO (Erbe-like TERRA ES8_Ed2)
N= 44 Model-Obs= 0.025 (0.021)